Relaxation of surface steps after thermal quenches: A numerical study within the terrace-step-kink model

S. Bustingorry[1] and P. M. Centres[2]
[1]*CONICET, Centro Atómico Bariloche, 8400 San Carlos de Bariloche, Río Negro, Argentina*
[2]*Departamento de Física, Instituto de Física Aplicada, Universidad Nacional de San Luis-CONICET, Chacabuco 917, D5700HHW, San Luis, Argentina*
(Received 8 April 2011; published 25 July 2011)

We study the out-of-equilibrium relaxation of surface steps after thermal quenches using numerical simulations of the terrace-step-kink model for a vicinal surface. We analyze both single and interacting steps in a situation where the temperature is suddenly changed at a given quench time. We focus on a physically relevant range of temperatures and show that the relaxation of the roughness is compatible with a power-law behavior with an effective relaxation exponent close to $\gamma = 1/2$ in all cases. This value is consistent with a one-dimensional Edwards-Wilkinson equation. In particular, this means that, although the case of interacting steps is effectively a two-dimensional system, its relaxation is dominated by short length-scale fluctuations, where steps are not interacting.

DOI: 10.1103/PhysRevE.84.011613 PACS number(s): 81.15.Aa, 68.35.Ct, 05.70.Np

I. INTRODUCTION

The understanding of the dynamics of solid-state surfaces is fundamental for a range of physical and chemical processes such as surface growth, chemical reactions, melting, and surface stability, among others. Beyond the idealized crystallographic surface, one should consider nonideal situations containing surface steps, impurities, or adatoms in order to gain a deep understanding of the problem. In particular, surface-step fluctuations and adatom diffusion in vicinal surfaces are key features that need to be tackled.

The equilibrium dynamics of vicinal surfaces has long been studied in different contexts [1,2]. It is well established now that this problem belongs to the universality class of the Edwards-Wilkinson (EW) equation, originally proposed for surface growth phenomena [3,4]. On the one hand, small-angle vicinal surfaces, where each step is independent of each other, correspond to a situation where two-point spatial correlations along the step diverge with the distance with the characteristic power-law behavior of the one-dimensional EW equation. On the other hand, when interactions among consecutive surface steps come into play, the system of steps becomes two-dimensional with large distance correlations logarithmically growing in both the direction along and perpendicular to the surface step. This is the behavior found in the two-dimensional EW equation, which is indeed in its critical dimension, and thus giving place to logarithmic correlations at large distances.

In contrast to the equilibrium situation, the out-of-equilibrium dynamics of vicinal surfaces has recently attracted renewed attention [5–9]. In particular, the experimental study of thermal quenches on oxide surfaces has shown the relevance of properly considering initial conditions and how it modifies the expected power-law behavior with time [9]. In addition, careful studies of the out-of-equilibrium properties of the EW equation has also been conducted [10–13]. One can notice in these works that the out-of-equilibrium dynamics can be investigated through the definition of different observables, each leading to complementary information.

It is interesting to notice the different power-law relaxation behaviors found after a sudden change of the growth conditions of the EW equation. This can be performed by changing the temperature or the stiffness of the system, and we will in general refer to this sudden change as a *quench*. The resulting relaxation depends on the time at which the quench is performed. By monitoring the response of the global roughness of the system, four different relaxation regimes separated by crossovers have been identified by Chou, Pleimling, and Zia [12]. If the quench is performed at extremely long times, where the saturation regime is dominant, exponential relaxation is expected. If the time of the quench is too short, it just adapts to the final condition too quickly and the relaxation of the system is too fast to be observable. For intermediate regimes, i.e., if the quench is performed in the growing regime where the correlation length is smaller than the size of the system, the relaxation of the roughness of the systems is expected to decay as a power law $t^{-\gamma}$, with two different effective relaxation exponents $\gamma = 1/2$ and $3/2$ depending on the quench conditions.

In the present work we test, using numerical simulations of the terrace-step-kink (TSK) model, whether these exponents can be observed in a vicinal surface problem, which belongs to the EW universality class. We perform simulations using a two-times protocol where the temperature is suddenly changed at a given quench time. We study both the single-step fluctuations and the case where interacting steps are considered. We have found that for parameters relevant to experimental situations the effective relaxation exponent is close to the value $\gamma = 1/2$, and we argue that the value $\gamma = 3/2$ would be difficult to be observed in the relaxation of vicinal surfaces since the necessary temperature difference at the quench is too large. The rest of the manuscript is organized as follows. In Sec. II we define the TSK model used here and give the main parameters of our simulation study. In Sec. III we give the definition of the quench protocol and the relevant observables used in this work, and in Sec. IV we present the main results concerning the relaxation exponent. Finally, Sec. V is devoted to concluding remarks.

II. TERRACE-STEP-KINK MODEL

The TSK model has long been used to study vicinal surfaces properties [5,14–18]. We briefly describe its main characteristics here. We consider a discrete model for the vicinal surface that for simplicity is defined on a square lattice with unit lattice constant and periodic boundary conditions in both directions. The longitudinal step size, in the $\hat{y}$ direction, is L, and the system contains N steps separated by an average distance ℓ, with the transverse size, in the $\hat{x}$ direction, given by $M = N\ell$. The position of the nth step is given by $x_n(y)$, and its deviation from its average position is given by

$$u_n(y) = x_n(y) - \frac{1}{L}\sum_{y=0}^{L-1} x_n(y). \tag{1}$$

In the TSK model the only allowed thermal excitations are kinks of energy ϵ, therefore neglecting adatoms and vacancies in the surface. It is also considered that steps are described by a single valued function $x_n(y)$, not allowing the formation of overhangs. In this model, the stiffness of an isolated step is

$$\widetilde{\beta} = 2k_BT \sinh^2\left(\frac{\epsilon}{2k_BT}\right). \tag{2}$$

For large temperatures such that $2k_BT \gg \epsilon$ the stiffness of isolated steps becomes $\widetilde{\beta} \sim \epsilon^2/(2k_BT)$. This is reminiscent of the behavior recently encountered in a model system closely related to the EW equation where the temperature dependence of the effective elasticity has been fitted to $\nu = (a + bT)^{-1}$ with a and b fitting parameters of order unity [13]. The large temperature behavior of the elasticity of this model is therefore $\nu \sim 1/T$ as in the TSK model, Eq. (2). This relation between elasticity and temperature has also recently been used to model fluctuations in vicinal surfaces using the EW equation [9], as suggested by earlier work [15–17,19]. Therefore, the generic property that $\nu \sim 1/T$ in all these models gives us a link between the temperature quenches we are studying and the results where the elasticity has suddenly changed in the EW equation [12,13].

Entropic repulsion is introduced in the TSK model through the nontouching (fermionic) constraint, requiring $x_n(y) < x_{n+1}(y)$ for all y. In addition to this entropic repulsion term, there is a term due to elastic repulsion, proportional to $A[x_{n+1}(y) - x_n(y)]^{-2}$, which for simplification is limited to neighboring steps. The Hamiltonian of the system is then given by

$$H = \epsilon \sum_{n=0}^{N-1}\sum_{y=0}^{L-1} |u_n(y+1) - u_n(y)| + A\sum_{n=0}^{N-1}\sum_{y=0}^{L-1} \frac{1}{[u_{n+1}(y) - u_n(y) + \ell]^2}, \tag{3}$$

with the additional nontouching constraint to be considered. With this model, we perform standard Monte Carlo numerical simulations with the Metropolis algorithm. Although kinetic Monte Carlo would be more reliable than the Metropolis algorithm when comparing time scales, for the present model these two numerical protocols give qualitatively the same information [6–8]. When one wants to directly compare among different time scales, kinetic Monte Carlo simulations would be preferable, as acknowledged in Refs. [7,8] when comparing relaxation times of surface steps with a Fokker-Planck time scale. Since we are not directly measuring time scales but presenting a general picture for the relaxation of surface steps we prefer to use the simple Metropolis algorithm.

As a reference temperature we consider the value $k_BT/\epsilon = 0.2$, which is a typical temperature scale encountered in copper vicinal surfaces [20,21]. For the quench protocols we will therefore use temperature changes between the values $k_BT/\epsilon = 0.2$, 0.5, and 1.0, which correspond to physically meaningful values. In experimental conditions, while smaller temperatures prevent step fluctuations, much larger temperatures would induce new mechanisms for particle motion, like the formation of vacancies and adatom diffusion on terraces.

A fundamental parameter of the model is the longitudinal collision length defined as [15]

$$y_{\mathrm{coll}} = \frac{\ell^2}{2}\sinh^2\left(\frac{\epsilon}{2k_BT}\right), \tag{4}$$

which gives the characteristic distance between close approaches among consecutive steps at a given temperature. For length scales smaller than y_{coll} surface steps fluctuate independently of each other. Here y_{coll} is the typical length at which collisions between consecutive steps can be observed. Therefore, for length scales larger than y_{coll} the fluctuations of the different steps are correlated.

We present results in this work with the longitudinal size $L = 512$. First, we will present data corresponding to independent single steps, which were obtained with $N = 64$ steps an average distance $\ell = 128$ apart (since steps are independent, the use of $N = 64$ improves statistical averages). For $k_BT/\epsilon = 1$ this amounts to $y_{\mathrm{coll}} \approx 2200 > L$, thus effectively corresponding to independent steps for this and smaller temperatures. We also use a system with $N = 256$ steps and $\ell = 4$ that for $k_BT/\epsilon = 0.2$ corresponds to $y_{\mathrm{coll}} \approx 300 < L$, giving an interacting-steps array for this and larger temperatures. In addition, in this last case we consider the elastic interaction term with intensity $A = 2$. Finally, we will also consider a case with $N = 128$, $\ell = 32$, and two temperature values, $k_BT/\epsilon = 0.2$ and $k_BT/\epsilon = 2$. For these values the corresponding collision lengths are $y_{\mathrm{coll}} \approx 18\,000$ and $y_{\mathrm{coll}} \approx 30$, respectively. This interesting case will therefore correspond to the case of thermal quenches between interacting and independent steps conditions. Finally, Monte Carlo numerical simulation data were averaged between 10^2 and 10^3 Monte Carlo runs, and time is given in units of Monte Carlo steps.

It can be shown that a coarse grain of the TSK model can be recast as an effective two-dimensional anisotropic EW equation with an additional term related to the discreteness of the model [19,22]. Since this is essentially a two-dimensional model, the EW equation is at its critical dimension ($d = 2$), and correlations grow logarithmically at large distances. However, if the average step separation ℓ is large enough so that the collision length is large compared with the relevant longitudinal size, the two-dimensional EW equation can be decoupled in N independent one-dimensional EW equations. In this case correlations grow as a power law with a characteristic exponent. Furthermore, since one expects the

effective elasticity term of the longitudinal EW equation to be approximately inversely proportional to the temperature, as mentioned before, thermal quenches will be directly reflected in a change of the parameter $\mu = \nu_i/\nu_f \sim T_f/T_i$ that controls the different relaxation regimes of the EW equation [12].

III. PROTOCOL AND OBSERVABLES

In the following we use the standard two-times protocol. The starting point is always the same "flat" initial condition, which means that the system of steps is in a perfect staircase configuration where all steps are straight and separated a distance ℓ. First, the system is let to evolve under a fixed initial temperature T_i. Then the temperature is suddenly changed to the final value T_f at the quench time s, and the system continues evolving. In order to monitor how the system relaxes to achieve equilibrium at the final temperature T_f, the global average roughness is computed as a function of t and s. This is given by

$$W^2(t,s) = \frac{1}{LN}\sum_{y=0}^{L-1}\sum_{n=0}^{N-1}\left[x_n(y) - \frac{1}{L}\sum_{y'=0}^{L-1} x_n(y')\right]^2, \qquad (5)$$

where $x_n(y)$ is a time-dependent quantity and s stands for the moment at which the system is perturbed. This roughness is compared with the one obtained with $s = 0$, which corresponds to the evolution from the initial flat configuration to equilibrium at given T_f and is considered the reference curve for a given quench protocol. With these computed quantities the desired relaxation roughness is obtained as

$$\Delta W^2(\Delta t,s) = |W^2(t,s) - W^2(t,0)|, \qquad (6)$$

with $\Delta t = t - s$ the elapsed time since the quench was performed and assuming $t > s$. Since we are trying to test power-law-type relaxation in the two-time quantity $\Delta W^2(\Delta t,s)$, we will evaluate the effective relaxation exponent defined through

$$\gamma(\Delta t) = -\frac{\partial \log \Delta W^2(\Delta t,s)}{\partial \log \Delta t}. \qquad (7)$$

One can analyze both longitudinal, along the step edge, and transverse fluctuations of steps. The latter give important information when the surface steps are close and interact with each other. Analogously to the longitudinal case, Eq. (5), the transverse global roughness is defined as

$$W_t^2(t,s) = \frac{1}{LN}\sum_{y=0}^{L-1}\sum_{n=0}^{N-1}\left[x_n(y) - \frac{1}{N}\sum_{n'=0}^{N-1} x_{n'}(y)\right]^2. \qquad (8)$$

One can then define the transverse relaxation roughness analogously in order to obtain ΔW_t^2 and then the effective relaxation exponent in the transverse direction, $\gamma_t(\Delta t)$. In spite of the fact that transverse fluctuations in vicinal surfaces [15–17,19,23] had attracted much less attention than the longitudinal ones, we think it is important to show similarities and differences among them. For example, although the TSK model can be shown to be described by the anisotropic two-dimensional EW equation, we found that the relaxation properties in the longitudinal and transverse directions are qualitatively similar and described by the same relaxation properties.

In Refs. [12,13] the evolution of the relaxation roughness $\Delta W^2(\Delta t,s)$ has been recently studied for the EW equation,

$$\frac{\partial x(\mathbf{y},t)}{\partial t} = \nu\nabla^2 x(\mathbf{y},t) + \eta(\mathbf{y},t), \qquad (9)$$

where $x(\mathbf{y},t)$ can be thought of a time-dependent height field in a d-dimensional substrate with coordinate $\mathbf{y}$, the noise $\eta(\mathbf{y},t)$ has zero average and correlations $\langle\eta(\mathbf{y},t)\eta(\mathbf{y}',t')\rangle = D\delta^d(\mathbf{y}-\mathbf{y}')\delta(t-t')$, and the parameter ν stands for the elasticity of the model, which drives the height field to a flat configuration. For this model, the evolution of the relaxation roughness can be generically described with a power law of the elapsed time $\Delta t = t - s$ since the quench was performed:

$$\Delta W^2(\Delta t,s) \sim \Delta t^{-\gamma}. \qquad (10)$$

The value of the relaxation exponent depends only on three scaling variables, namely, $\mu = \nu_i/\nu_f$, $\sigma = \nu_f s$, and $\rho = t/s$, where $\nu_f(\nu_i)$ are the elasticity after (before) the quench. Depending on these parameters and considering also the dimension d of the EW equation, the relaxation exponent can take different values. The value $\gamma = 0$ is typically expected at very short time scales, either $\nu_f s \ll 1$ or $\nu_f(t-s) \ll 1$. On the contrary, at very long time scales, $\nu_f s \gg 1$ or $\nu_f(t-s) \gg 1$, exponential relaxation is observed instead of the power-law behavior, Eq. (10). At intermediate time scales the parameter μ typically separates two regimes according to

$$\gamma = \begin{cases} 1 + \frac{d}{2} & \text{for} \quad \mu \ll 1, \\ \frac{d}{2} & \text{for} \quad \mu \gg 1. \end{cases} \qquad (11)$$

Since in the vicinal surface problem one expects that $\nu \sim 1/T$, the value of $\mu \sim T_f/T_i$ controls the relaxation of the roughness at intermediate time scales, typically encountered in experiments. In the following we test the values of the relaxation exponent in the TSK model.

IV. RESULTS

A. Independent steps

We present in this section the numerical results obtained using the TSK model with the quench protocol. We start with the analysis of the data corresponding to single independent steps. Figure 1 shows the evolution of the roughness for constant temperatures $T = 1\epsilon/k_B$ and $T = 0.2\epsilon/k_B$, circles and squares, respectively. It is clear that the data corresponding to the roughness for $T = 1\epsilon/k_B$ show the three typical regimes of the EW growth equation: (1) a random deposition regime for very short time $t \ll t_1$, i.e., $W^2 \sim t$, (2) correlated growth regime $W^2 \sim t^{2\beta}$ for $t_1 \ll t \ll t_2$ with the characteristic growing exponent $\beta = 1/4$, and (3) system size-dependent saturation $W^2 \sim L^{2\alpha}$ for $t \gg t_2$ with the roughness exponent $\alpha = 1/2$. These three regimes are highlighted with dashed lines in Fig. 1 for $T = 1\epsilon/k_B$. In the case corresponding to $T = 0.2\epsilon/k_B$ (squares), the two crossover times are too close, $t_1 \approx t_2$, and therefore the intermediate correlated grow regime becomes a wide crossover between random deposition and saturation. It is also shown in Fig. 1 the results for a quench protocol from $T_i = 1\epsilon/k_B$ to $T_f = 0.2\epsilon/k_B$ at the quench time $s = 10^2$ (blue diamonds). After the sudden quench the roughness relax trying to reach equilibrium at T_f.

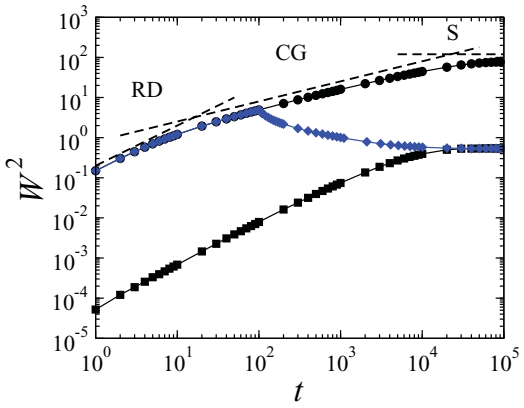

FIG. 1. (Color online) Time evolution of the global roughness for the TSK model. Full circles (squares) correspond to the evolution from an initial flat configuration at a temperature $T = 1\epsilon/k_B$ ($T = 0.2\epsilon/k_B$). Full diamonds correspond to the evolution from an initial flat condition at $T_i = 1\epsilon/k_B$ but with a sudden quench to $T_f = 0.2\epsilon/k_B$ at the quench time $s = 10^2$. Dashed lines highlight the three expected regimes in the one-dimensional EW equation: random deposition (RD), correlated growth (CG), and saturation (S).

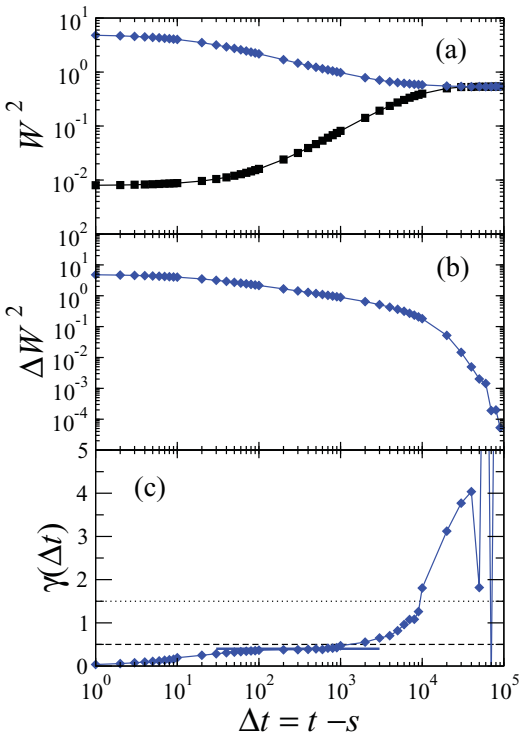

FIG. 2. (Color online) (a) Evolution of the global roughness with the elapsed time since the quench, $\Delta t = t - s$. Full squares correspond to the evolution since the quench at the reference final temperature $T = 0.2\epsilon/k_B$, and full diamonds correspond to the quench protocol from $T_i = 1\epsilon/k_B$ to $T_f = 0.2\epsilon/k_B$. (b) Evolution of $\Delta W^2(\Delta t)$, corresponding to the difference between the quenched and the reference data in (a). (c) The effective relaxation exponent defined through the logarithmic derivative of ΔW^2 Eq. (7). As a reference, we also plot the values $\gamma = 1/2$ (dashed line) and $\gamma = 3/2$ (dotted line) expected for the one-dimensional EW case.

The same data reported in Fig. 1 are shown in Fig. 2(a) but as a function of the elapsed time Δt, which is used to construct the relaxation roughness defined in Eq. (6), as shown in Fig. 2(b). In order to obtain the effective relaxation exponent, Eq. (7), we evaluate numerically the forward difference of the data in Fig. 2(b). The obtained evolution of the effective relaxation exponent with the elapsed time, $\gamma(\Delta t)$, is reported in Fig. 2(c). The values $\gamma = 1/2$ (dashed line) and $\gamma = 3/2$ (dotted line), which are the expected steady values for the relaxation exponent of the one-dimensional EW equation, are also shown in Fig. 2(c) as reference values. After a transient time, which is of the order of the quench time s, the relaxation exponent shows a steady value that is indicated with a bold continuous line in the figure and is close to $\gamma = 1/2$. After that, the value of the relaxation exponent grows and finally develops strong fluctuations when $\Delta W^2(\Delta t) \to 0$. The observed final increase of γ_t is related to the final exponential relaxation expected at very long times [12]. The observed steady value compares well with the EW results $\gamma = 1/2$. Although the results presented here are for $L = 512$, we have checked that the value of the steady effective relaxation exponent does not depend much on the system size for the same quench protocol.

Figure 3 reports the effective relaxation exponent for different quench protocols: (a) $T_i = 1\epsilon/k_B$ to $T_f = 0.2\epsilon/k_B$ [same data as in Fig. 2(c)], (b) $T_i = 0.5\epsilon/k_B$ to $T_f = 0.2\epsilon/k_B$, and (c) inverse quench protocol from $T_i = 0.2\epsilon/k_B$ to $T_f = 1\epsilon/k_B$. The quench time is $s = 10^2$ in all cases. One can observe in Figs. 3(a) and 3(b) that the steady value of the effective relaxation exponent seems to be slightly changing with T_f/T_i. In fact, as discussed in Sec. III, a key parameter controlling the value of the relaxation exponent in the EW equation is the quotient of the initial and final elasticity, $\mu = \nu_i/\nu_f \sim T_f/T_i$. As shown in Ref. [12], in the crossover regions between the different values of γ, a small change of

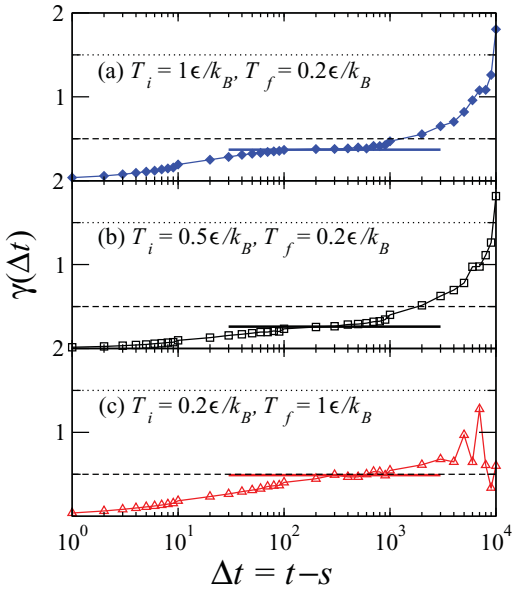

FIG. 3. (Color online) Effective relaxation exponent obtained in different quench protocols as indicated in the keys, all with a quench time $s = 10^2$. As a reference, we also plot the values $\gamma = 1/2$ (dashed line) and $\gamma = 3/2$ (dotted line) expected for the one-dimensional EW case.

the relaxation exponent with μ can be observed at a fixed value of the quench time s. The data reported in Fig. 3(c) correspond to the case where the quench time s is too short compared with the crossover time t_1, as can be observed in the evolution of the roughness for $T_f = 0.2\epsilon/k_B$ in Fig. 1. Although in this case one would expect an effective exponent $\gamma = 0$ for the EW equation [12], our numerical results suggest that the steady value of γ might be around $1/2$. This can be also a result of the final state being at a larger temperature and thus in a correlated grow regime at the quench time.

We have therefore shown that our results for the relaxation of single steps are consistent with the analytical results obtained for the one-dimensional EW equation. However, in the parameter space used here, we have not observed a relaxation exponent close to $\gamma = 3/2$. This value would be observable for $\mu \sim T_f/T_i \ll 1$ [12], which corresponds to a quench to a final temperature much smaller than the initial one. This could be achieved with a very large initial temperature, where adatoms and vacancy diffusion would destroy the image of a parallel step array considered in the TSK model, or with a very small final temperature where steps do not fluctuate within observable time scales. Therefore, we do not expect the value $\gamma = 3/2$ to be observed in the physically relevant temperature range for the TSK model studied here.

B. Interacting steps

We present here results corresponding to the case of interacting steps in a vicinal surface. In this case longitudinal and transverse fluctuations can be considered. For illustration purposes we show here only results corresponding to transverse fluctuations, the longitudinal case being qualitatively similar. The interacting-steps system can be related to a two-dimensional EW growth equation, which is therefore in its critical dimension ($d = 2$). It is expected that in this case correlations grow logarithmically and not as a power law. In fact, as can be observed in Fig. 4 for constant $T = 1\epsilon/k_B$ and flat initial condition the intermediate correlated grow regime is not present, as in Fig. 1, but a logarithmic growing regime seems to be present. In the case with $T = 0.2\epsilon/k_B$ and flat initial condition the intermediate logarithmic grow is not reached and saturation is rapidly developed. Blue diamonds in Fig. 4 correspond to the quench from $T_i = 1\epsilon/k_B$ to $T_f = 0.2\epsilon/k_B$ at $s = 10^3$. The quench is therefore initiated in the growing regime of the initial temperature but in the saturation regime of the final temperature. As can be observed, a key difference with the results reported in Fig. 1 is that in the interacting-steps case the relaxation has two characteristic stages. A fast initial decay is followed by a second slower relaxation, which results in the shoulder observed in the global relaxation after the quench. The reason for this two-stage behavior could be that the initial relaxation is modified by the existence of the transverse analog of the longitudinal collision length $y_{\rm coll}$. This two-stage behavior is also present when analyzing the longitudinal relaxation of the interacting-steps system.

In Fig. 5(a) we show numerical results corresponding to the transverse relaxation roughness ΔW_t^2 as a function of the elapsed time Δt in the TSK model with $L = 512$, $N = 256$, $\ell = 4$, and $A = 2$. We show the quench from $T_i = 1\epsilon/k_B$ to $T_f = 0.2\epsilon/k_B$ (squares) and the inverse quench from $T_i = 0.2\epsilon/k_B$ to $T_f = 1\epsilon/k_B$ (triangles), both at the quench time $s = 10^3$. From these data, we obtained the transverse effective relaxation exponent shown in Fig. 5(b). Although it is not that clear that γ_t has reached the steady value, it seems that a plateau is developing around $\gamma_t \approx 0.3 < 1/2$ [bottom straight line in Fig. 5(b)], for both the direct and inverse quench protocols. We think this is related to the first stage in the relaxation observed in Fig. 4. A careful inspection of the data for γ_t reveals that it also accounts for the shoulder observed in the evolution of the global transverse roughness after the quench, as shown in

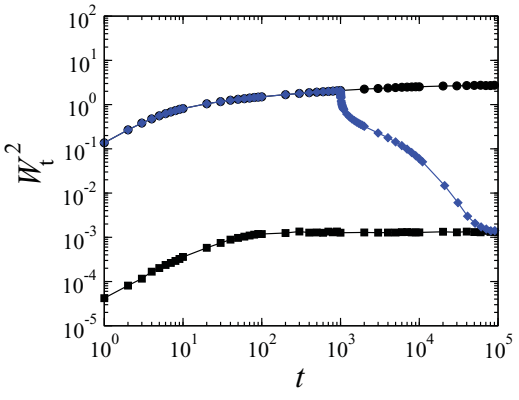

FIG. 4. (Color online) Time evolution of the global roughness for the TSK model in the case of interacting steps where the average distance between consecutive steps is $\ell = 4$ and the interaction strength is $A = 2$. Full circles (squares) correspond to the evolution from an initial flat configuration at a temperature $T = 1\epsilon/k_B$ ($T = 0.2\epsilon/k_B$). Full diamonds correspond to the evolution from an initial flat condition and at $T_i = 1\epsilon/k_B$ but with a sudden quench to $T_f = 0.2\epsilon/k_B$ at the quench time $s = 10^3$.

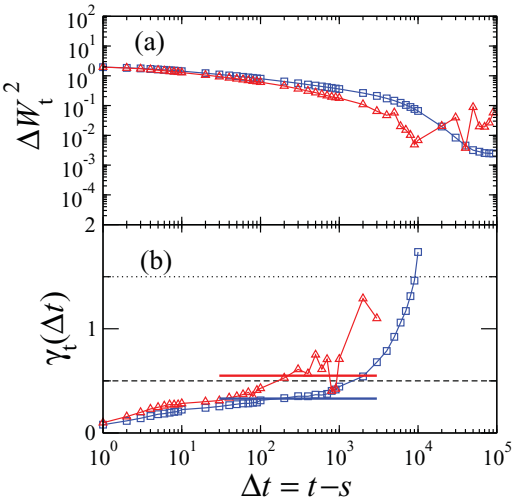

FIG. 5. (Color online) Transverse fluctuations of interacting steps for the TSK model with $L = 512$, $N = 256$, $\ell = 4$, and $A = 2$. (a) Transverse relaxation roughness for the case of interacting steps. Squares correspond to the direct quench from $T_i = 1\epsilon/k_B$ to $T_f = 0.2\epsilon/k_B$, and triangles correspond to the inverse quench from $T_i = 0.2\epsilon/k_B$ to $T_f = 1\epsilon/k_B$, both at the quench time $s = 10^3$. (b) Transverse effective relaxation exponent for the data in (a).

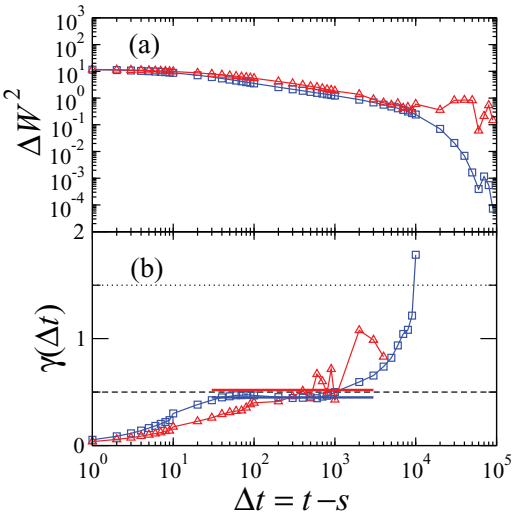

FIG. 6. (Color online) Longitudinal fluctuations of interacting steps for the TSK model with $L = 512$, $N = 128$, $\ell = 32$, and $A = 0$. The two temperatures considered here corresponds to the case of interacting steps, $T = 2\epsilon/k_B$, and single steps, $T = 0.2\epsilon/k_B$. (a) Evolution of the relaxation roughness since the quench at $s = 10^2$. Squares correspond to the direct quench from $T_i = 2\epsilon/k_B$ to $T_f = 0.2\epsilon/k_B$, and triangles correspond to the inverse quench from $T_i = 0.2\epsilon/k_B$ to $T_f = 2\epsilon/k_B$. (b) Effective relaxation exponent for the data in (a).

Fig. 4. For the inverse quench the data seem to develop a second steady state at a value slightly larger than 1/2 [upper straight line in Fig. 5(b)]. However, the data for the direct quench show a relaxation that is consistent with an exponential behavior for the second stage. We therefore conclude that although the origin of the second stage of the relaxation in Fig. 4 is not clear and might be related to transverse fluctuations, the two-stage relaxation can be observed in the behavior of the effective relaxation exponent. Besides, we think that this two-stage relaxation makes it difficult to reach a steady value for the effective relaxation exponent.

Since the parameter $y_{\rm coll}$, indicating whether the system is in the interacting regime or not, depends on temperature, we finally report in Fig. 6 results for the especial case where the quench is made between two temperatures corresponding to the system in the single-steps regime and in the interacting-steps regime, respectively. In this case we use the TSK model with $L = 512$, $N = 128$, $\ell = 32$, and $A = 0$. The two temperatures studied were $T = 2\epsilon/k_B$ and $T = 0.2\epsilon/k_B$, which yields $y_{\rm coll} \approx 18\,000$ and 30, respectively. In Fig. 6(a) the longitudinal relaxation roughness ΔW^2 is shown with the corresponding effective relaxation exponent in Fig. 6(b). Again, the steady value of γ seems to be close to $\gamma = 1/2$ for both quench protocols.

Although the value of the effective relaxation exponent of the EW equation depends on the considered dimension [13], Eq. (11), we have always quoted the values corresponding to the one-dimensional case, even in the interacting-steps case which corresponds to two dimensions. The reason for this is that the two-dimensional character is expected to be effectively observable at very large distances, much larger than the longitudinal collision length. Notice that the expected values for the relaxation exponents in d dimensions, Eq. (11), are larger than the value $\gamma = d/2$, which is close to our numerical results. This means that we never observe γ close to the smaller value expected in two dimensions, and therefore that fluctuations on scales of the order of $y_{\rm coll}$ dominate the relaxation in the cases studied here.

V. CONCLUDING REMARKS

We have performed here numerical simulations of the TSK model for vicinal surfaces focusing on the response of the system to a quench protocol. We have analyzed a particular physically relevant temperature range. The study of the relaxation roughness, which measures the difference between the quenched roughness and the final reference state, gives information on the relaxation of the system, contained in the effective relaxation exponent γ. In the range of parameters we have used, the steady value of γ is always close to the value $\gamma = 1/2$. A first important conclusion of our results is that the value $\gamma = 3/2$ would be hardly observable in experiments. It would be necessary to perform a quench with the final temperature at least two orders of magnitude smaller than the initial temperature in order to observe $\gamma = 3/2$. Finally, we should also remark that for the parameters studied here, the fact that the effective relaxation exponent is close to $\gamma = 1/2$ for the case of interacting steps is indicating that the relevant fluctuations for the relaxation of the system are those at scales smaller that the longitudinal collision length. In addition, our results are showing that the expected behavior in the simple one-dimensional EW case can be extrapolated to more involved situations, the TSK model being a non-trivial EW type of system, with the elasticity depending on temperature.

ACKNOWLEDGMENTS

We would like to thank stimulating correspondence with M. Pleimling. This work was supported in part by CONICET (Argentina) under project numbers PIP 112-200901-00051 and PIP 112-200801-01332, Universidad Nacional de San Luis (Argentina) under project 322000, and the National Agency of Scientific and Technological Promotion (Argentina) under project 33328 PICT 2005.

[1] M. Giesen, Prog. Surf. Sci. **68**, 1 (2001).
[2] C. Misbah, O. Pierre-Louis, and Y. Saito, Rev. Mod. Phys. **82**, 981 (2010).
[3] S. F. Edwards and D. R. Wilkinson, Proc. R. Soc. London A **381**, 17 (1982).
[4] A.-L. Barábasi and H. E. Stanley, *Fractal Concepts in Surface Growth* (Cambridge University Press, Cambridge, UK, 1995).
[5] E. Le Goff, L. Barbier, and B. Salanon, Surf. Sci. **531**, 337 (2003).

[6] A. Pimpinelli, H. Gebremariam, and T. L. Einstein, Phys. Rev. Lett. **95**, 246101 (2005).
[7] A. B. Hamouda, A. Pimpinelli, and T. L. Einstein, J. Phys. Condens. Matter **20**, 355001 (2008).
[8] A. B. Hamouda, A. Pimpinelli, and T. L. Einstein, Surf. Sci. **602**, 3569 (2008).
[9] T. T. T. Nguyen, D. Bonamy, L. Phan Van, J. Cousty, and L. Barbier, Europhys. Lett. **89**, 60005 (2010).
[10] A. Röthlein, F. Baumann, and M. Pleimling, Phys. Rev. E **74**, 061604 (2006).
[11] S. Bustingorry, L. F. Cugliandolo, and J. L. Iguain, J. Stat. Mech.: Theor. Exp. P09008 (2007).
[12] Y.-L. Chou, M. Pleimling, and R. K. P. Zia, Phys. Rev. E **80**, 061602 (2009).
[13] Y.-L. Chou and M. Pleimling, J. Stat. Mech.: Theor. Exp. P08007 (2010).
[14] N. C. Bartelt, T. L. Einstein, and E. D. Williams, Surf. Sci. **240**, L591 (1990).
[15] N. C. Bartelt, T. L. Einstein, and E. D. Williams, Surf. Sci. **276**, 308 (1992).
[16] L. Masson, L. Barbier, J. Cousty, and B. Salanon, Surf. Sci. **317**, L1115 (1994).
[17] E. Le Goff, L. Barbier, L. Masson, and B. Salanon, Surf. Sci. **432**, 139 (1999).
[18] H. Gebremariam, S. D. Cohen, H. L. Richards, and T. L. Einstein, Phys. Rev. B **69**, 125404 (2004).
[19] L. Barbier, L. Masson, J. Cousty, and B. Salanon, Surf. Sci. **345**, 197 (1996).
[20] M. Giesen and T. L. Einstein, Surf. Sci. **449**, 191 (2000).
[21] H. L. Richards, S. D. Cohen, T. L. Einstein, and M. Giesen, Surf. Sci. **453**, 59 (2000).
[22] J. Villain, D. R. Grempel, and J. Lapujoulade, J. Phys. F **15**, 809 (1985).
[23] A. N. Benson, H. L. Richards, and T. L. Einstein, Phys. Rev. B **73**, 115429 (2006).